Journal of Bioprocessing & Biotechniques

Hejazi et al., J Bioprocess Biotech 2015, 5:4
DOI: 10.4172/2155-9821.1000219

Research Article Open Access

Effect of Alumina Amount on the Bioactivity of Dense Magnesium Fluorapatite/Alumina Composite in Simulated Body Fluid (SBF) using Taguchi Method

Hejazi MS[1,2*], Meratian M[1], Ahmadian M[1,2] and Fathi MH[1,3]

[1]Department of Materials Engineering, Isfahan University of Technology, Isfahan, 84156-83111, Iran
[2]Biomaterials Research Group, Department of Materials Engineering, Isfahan University of Technology, Isfahan, 8415683111, Iran
[3]Dental Materials Research Center, Isfahan University of Medical Sciences, Isfahan, Iran

Abstract

Bioactivity of magnesium fluorapatite is basically affected by the amount of dissolved β-TCP in Simulated Body Fluid (SBF). It was the purpose of the current work to prepare and characterize magnesium fluorapatite with different amounts of alumina, and to investigate the effect of alumina amount on magnesium fluorapatite (MFA) bioactivity and mechanical properties. Magnesium fluorapatite/alumina composite bulk samples with different amounts of alumina were synthesized via mechanochemical activation (by high-energy ball milling process) followed by two-step sintering processes using Taguchi method and analysis of variance (ANOVA). While, variable parameters include: initial temperature (T_1), second temperature (T_2) and dwell time (t_2). In vitro bioactivity evaluation was performed by soaking the prepared samples in Simulated Body Fluid (SBF) for predicted period of times. In order to characterize the samples, identify the formed bone like-apatite, and determine the concentration amount of released ions in the SBF, X-ray diffraction, Fourier transform infrared spectrometry, scanning electron microscopy, inductively-coupled plasma, and spectrometry techniques were utilized. The results indicated that the MFA/alumina composites with various amounts of alumina showed more bioactivity in SBF due to higher dissolution of β-TCP.

Keywords: Magnesium-fluorapatite; Bio composite; Bioactivity; Simulated body fluid; Two-step sintering; Taguchi method

Introduction

The use of Hydroxyapatite (HA) as an implant for bone replacement in restorative dental and orthopedic applications owes much to the similarity of its chemical composition and crystallographic structure to those of the bone mineral part; HA, however, suffers from poor mechanical properties [1,2]. It is possible to obtain improved mechanical properties such as strength, wear resistance, fracture toughness and hardness by combining HA with hard alumina [3-5]. In order to implant HA prostheses in the human body, it is essential to create bonding to a live bone similar to the apatite formed in a Simulated Body Fluid (SBF) [6,7]. The *in vivo* formation of apatite on bioactive ceramics can be reproduced by an acellular simulated body fluid (SBF) with ion concentrations nearly equal to those in the blood plasma [8]. The biologically active bone-like calcium-phosphate (Ca-P) layer is necessarily formed on the implant surface [9]. It is accepted that HA and β-TCP form chemical bonds directly with bone tissues without the intervention of soft tissues [10]. A number of studies have been conducted on the bioactivity of ceramic composites with alumina and/or HA. Zhang et al. [11] showed that Al_2O_3/diopside ceramic composites had both good mechanical properties and good biological activity. Priya et al. [12] observed that calcium phosphate-mullite composites were capable of producing a porous apatite layer *in vitro*. Xin et al. [13] investigated the apatite layer formation and found that it occurred on the surface of HA/316L SS biocomposites. Taguchi's approach is a method for improving the quality of a product through minimizing the effect of variation without eliminating the causes [14]. A typical two-step sintering schedule consists of a first heating step to an initial temperature (T_1) for short time (t_1) and, on a second step, the immediate cooling down to a lower temperature (T_2) for a relatively long time (t_2) [15]. The method was tested in a variety of materials, including alumina [16], alumina- zirconia [17] and hydroxyapatite [18]. ANOVA could be estimated the appropriate orthogonal array for experiments [19]. In the present work, the bioactivity, fracture toughness and hardness of MFA samples with various amounts of alumina (0, 10, 25, and 50 wt %) under a two-step sintering processes using Taguchi method in SBF is studied.

Materials and Methods

MFA/alumina composites were synthesized using ball milling. In order to obtain MFA powders, phosphorous pentoxide (P_2O_5), calcium hydroxide ($Ca(OH)_2$), magnesium hydroxide ($Mg(OH)_2$), and calcium fluoride (CaF_2) powders (all p.a, Merck) were mechanochemically activated using a high-energy planetary ball mill (Fretch Pulverisette-5, Germany) at ambient temperature for 12 hours. In order to obtain MFA/alumina composites with 10, 25 and 50 wt% alumina, α-Al_2O_3 (Aldrich, USA) was added to MFA and milled for 3 hours. A tension-compression of manufacturer device under a pressure of 300 MPa was used for the preparation of green pellets. Two-step sintering processes were designed and applied by Taguchi method for composites. In the Taguchi parameter design, three initial temperatures (1150, 1200 and 1250°C), three secondary temperature (1000, 1100 and 1150°C) and three dwell times (4, 8 and 12 hours) were selected. The bulk samples were evaluated with respect to their bioactivity using an SBF immersion test with features of the blood serum (i.e., pH=7.4 at 37°C) [7]. The bulked samples were immersed in SBF with different test characteristics.

***Corresponding author:** Hejazi MS, Department of Materials Engineering, Isfahan University of Technology, Isfahan, 84156-83111, Iran, Tel: 983-113-915-73; E-mail: ms.hejazi@ma.iut.ac.ir

Received March 03, 2015; **Accepted** Aprile 07, 2015; **Published** Aprile 13, 2015

Citation: Hejazi MS, Meratian M, Ahmadian M, Fathi MH (2015) Effect of Alumina Amount on the Bioactivity of Dense Magnesium Fluorapatite/Alumina Composite in Simulated Body Fluid (SBF) using Taguchi Method. J Bioprocess Biotech 5: 219 doi: 10.4172/2155-9821.1000219

In order to approve and confirm the bone-like apatite formation, Fourier Transform Infrared Spectrometer (FTIR), (Burker Tensor), was employed to identify the appearance of OH^-, PO_4^{3-}, and CO_3^{2-} in a wavelength range of 600 to 4000 cm^{-1}. The phases of the immersed MFA/alumina samples were determined using X-ray diffraction (Philips diffractometer (40 kV) with a $Cu_{K\alpha}$ radiation of 0.15406 nm). Inductively-Coupled Plasma (ICP), spectrometry (DV7300-Perkin Elmer) was employed to identify the ion concentration changes of the solutions during soaking in SBF. The formation and the growth of bone-like apatite on the soaked pellet surfaces over different immersion times were investigated using a scanning electron microscope (SEM, Phillips XL 30). Fracture toughness (K_{IC}) and hardness (Hv) were determined using the following equations [15]:

$K_{IC}=0.0824P/C^{3/2}$, $H_v=1.854P/d^2$

Where, P stands for applied load (N), C for crack length, d stands for the diagonal length of the indentation.

Results

Taguchi method

According to Chen and Wang reports [17], the success of two step sintering strongly depends on the choices of temperatures T_1 and T_2. In their experiment, a sample is sintered to the higher temperature T_1 to achieve a density higher than 75%, corresponding to a state in which all pores in the sample are unstable and shrinkable. It is reported that the MFA relative density was reached to 94% at 1050°C for 1 min by Hidouri et al. [20]. Therefore, TSS_1 process as below: T_1=1050, t_1=1min, T_2= 950 and t_2=20 h was applied for MFA only. TSS_2 processes were designed for composite samples followed by Taguchi method. To determine the initial temperature, conventional sintering for MFA composite with 50% alumina was performed at different temperatures from 1000 to 1300°C. The densities of composite samples are shown in Table 1. The temperature resulting in 75% of relative density and higher densities are suitable for the selection of the initial temperatures [15]. Figure 1a shows MFA composite sample with 50% alumina sintered at temperature of 1250°C. Alumina, MFA, β-TCP and calcium aluminate phases were observed. The higher sintering initial temperature as well as the higher alumina content in MFA/50% alumina composite is illustrating further decomposition of MFA into β-TCP and the $CaAl_2O_4$ formation. Figure 1b shows XRD pattern of MFA/50% alumina sintered at 1300°C. While temperature of 1300°C is resulting 79.5% of relative density (Table 1), MFA entirely decomposed into β-TCP (Figure 1). Because of this, temperatures of 1300°C or higher wasn't suitable for initial temperature. Table 2 presents the design of experiments by Taguchi method and the values of densities corresponding to each experiment. Three levels for each variable refer to the maximum and minimum limits that influence on the density of the final products.

The influential parameters which obtained from ANOVA analysis are listed in Tables 3, 4 and 5 for MFA composite samples with 10, 25 and 50% α-alumina, respectively. The most influential parameters are the initial temperature (T_1=68.809%) and secondary temperature (T_2=21.090), the initial temperature (T_1=26.745%) followed by dwell time (t_2=25.329) and secondary temperature (T_2=18.943), the initial temperature (T_1=62.669%) and dwell time (t_2=2.662), respectively. The highest influence on their relative density is related to T_1 because of its exponential form [21]. In addition to, alumina sintering is carried out in the high enough temperatures (range between 1400 to 1750°C) [22]. So, the sintering optimum conditions (TSS_2 process) as well as higher densification was obtained at higher initial temperature. Furthermore, at high temperature, grain boundary diffusion is active in removing pores, giving more densification [21]. A combination of $[(T_1)_2, (T_2)_3, (t_2)_2]$, $[(T_1)_2, (T_2)_3, (t_2)_3]$ and $[(T_1)_3, (T_2)_2, (t_2)_2]$ as the highest yield for MFA composite samples with 10, 25 and 50% alumina, respectively.

Sintering temperature (°C)	Density (%TD)
1000	69.0
1100	71.5
1200	75.0
1300	79.5

Table 1: Relative density and crystallite size for MFA composite with 50% alumina.

Exp. No	T_1(°C)	T_2(°C)	t_2(h)	10% alumina	25% alumina	50% alumina
1	1150	1000	4	81.19	80.30	74.39
2	1150	1050	8	82.51	80.35	74.83
3	1150	1100	12	83.03	83.16	74.11
4	1200	1000	8	83.43	82.76	75.31
5	1200	1050	12	84.28	84.32	75.74
6	1200	1100	4	86.09	83.00	74.75
7	1250	1100	12	79.94	82.62	75.63
8	1250	1050	4	79.61	80.65	75.56
9	1250	1100	8	82.22	84.11	76.31

Table 2: Design of experiments by Taguchi method accompany with the values of composites density corresponding to each experiment.

SBF behavior using TSS process.

Figures 2a-2d shows the FTIR observations of the composite samples after immersion in SBF for 28 days. The presence of wide bands in the range of 1000-1150 cm^{-1} is reportedly attributed to PO_4 vibrations. The absorption peaks located at 720, 1410-1490, and 1520-1560 were assigned to the CO_3 bands [23]. The band at 1670 cm^{-1} was attributed to H_2O bands and the characteristic peak at 3575 cm^{-1} was derived from the OH band [9]. The FTIR bands confirmed the development of phosphate and carbonate bands and, subsequently, the formation of the apatite layer on the composite surfaces by immersion in SBF for 28 days.

Figures 3a-3d shows XRD patterns for MFA/alumina composites after immersion in SBF for 28 days. The XRD patterns confirm the results obtained from FTIR analysis. The diffractions from the sample surfaces after the 28th day immersion in SBF show the presence of β-TCP and the formation of apatite on sample surfaces. The broadening of β-TCP and apatite peaks occurred due to alumina addition (Figure 4) since it indicates the formation of a non-crystallite phase on the sample surfaces. Furthermore, the decreasing β-TCP intensity with increasing alumina content indicates the excessive decomposition of SBF due to the dissociation of magnesium fluorapatite. The higher β-TCP solubility results in higher bioactivity and accelerates the growth rate of bone-like HA. It may be concluded that appetites associated with β-TCP exhibit a good biological response in SBF [6,10]. The changes in Ca and P ion concentrations in response to different immersion times are shown in Figures 5a-5c. The formation and growth of apatite corresponding to the dynamic process follow as the material surfaces dissolve and the apatite layers precipitate on the surface. The formation of apatite in SBF is expressed as follows [13]:

$$10\,Ca^{2+} + (6\text{-}X)\,PO_4^{3-} + 2OH^- + xCO_3^{2-} \rightarrow Ca_{10}(PO_4)_{6-x}(CO_3)_x(OH)_2 \quad (1)$$

Therefore, Ca ion concentration increases with the dissolution of the surface layer. Thus, it is believed that apatite nucleation and growth occur with Ca and P ion consumption. As seen during the test

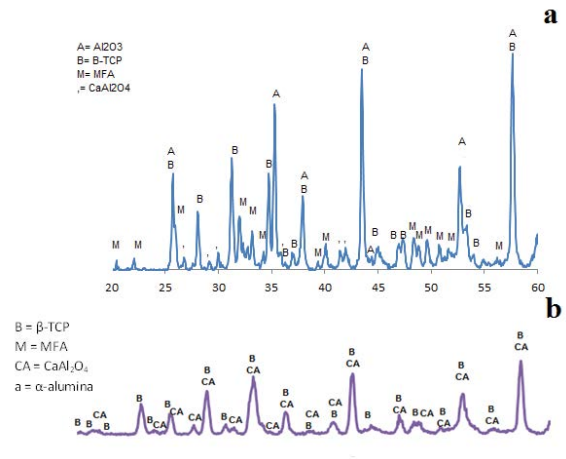

Figure 1: XRD pattern of MFA/50% alumina sintered at a) 1250°C and b) 1300°C.

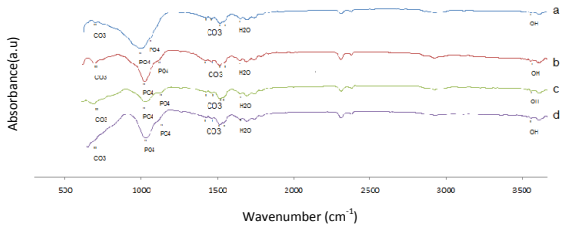

Figure 2: FTIR spectra of a) pure MFA, b) MFA/10% alumina, c) MFA/25% alumina and d) MFA/50% alumina after immersion in SBF for 28 days.

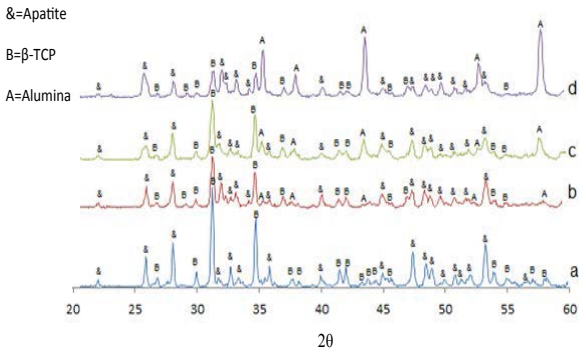

Figure 3: XRD patterns for a) MFA, b) MFA/10% alumina, c) MFA/25% alumina and d) MFA/50% alumina after immersion in SBF 28 days.

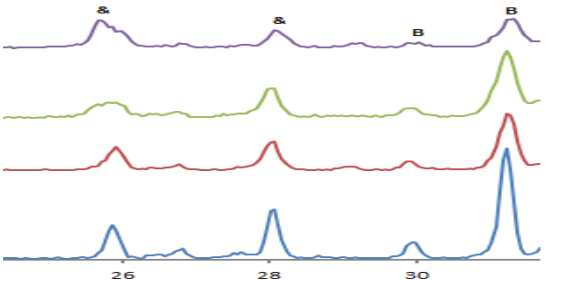

Figure 4: The Broadening of the β-TCP and apatite peaks.

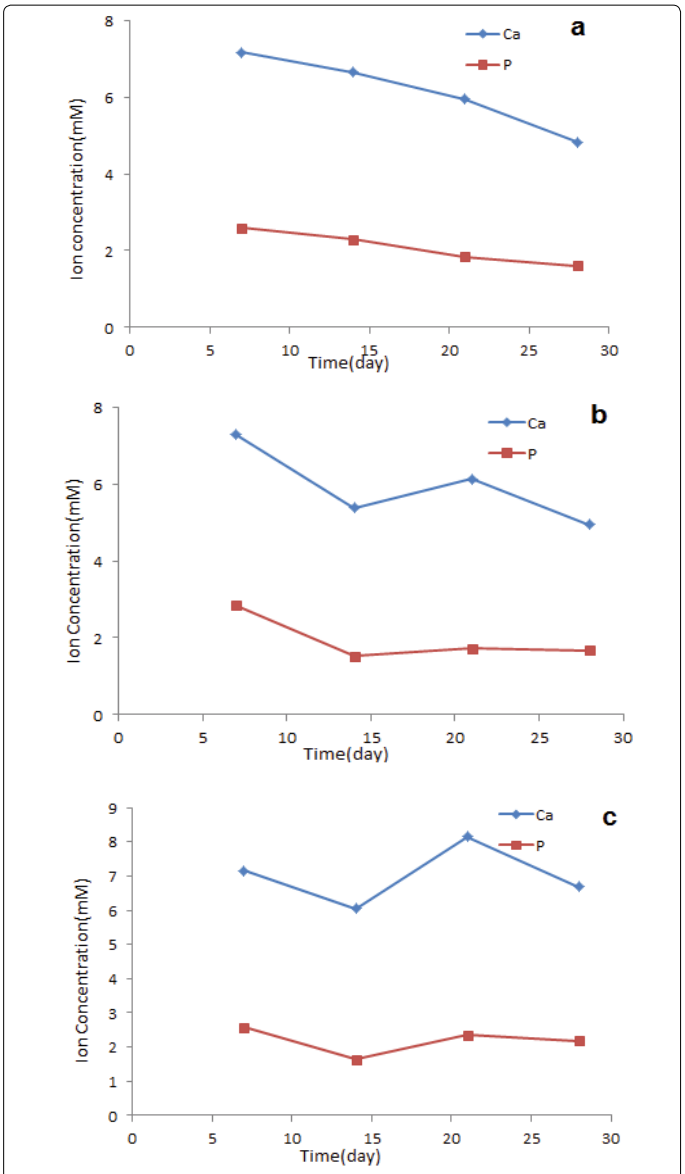

Figure 5: Ca and P ion concentrations changes with immersion time for a) MFA, b) MFA/25% alumina, and c) MFA/50% alumina in SBF.

Parameters	Sum of squares	Degrees of freedom	variance	Pure sum of squares	F-ratio	influence
T_1	24.371	2	12.185	23.35	23.299	68.809
T_2	8.195	2	4.097	7.149	7.834	21.090
t_2	0.285	2	0.142	---	0.273	0
Error/other.	1.045	2	0.522	---	---	10.101
Total	33.898	8	---	---	---	100

Table 3: ANOVA of the influential parameters for the MFA/10 % alumina.

Parameters	Sum of squares	Degrees of freedom	Variance	Pure sum of squares	F-ratio	influence
T_1	6.560	2	3.295	5.185	4.691	26.745
T_2	5.077	2	2.538	3.672	3.614	18.943
t_2	6.315	2	3.157	4.911	4.495	25.329
Error/other.	1.403	2	0.701	---	---	28.893
Total	19.388	8	---	---	---	100

Table 4: ANOVA of the influential parameters for the MFA/25% alumina.

Parameters	Sum of squares	Degrees of freedom	Variance	Pure sum of squares	F-ratio	influence
T_1	2.933	2	1.466	2.526	7.200	62.669
T_2	0.175	2	0.087	---	0.430	0
t_2	0.514	2	0.257	0.107	1.263	2.662
Error/other.	0.406	2	0.203	---	---	34.669
Total	4.030	8	---	---	---	100

Table 5: ANOVA of the influential parameters for the MFA/50% alumina.

Composite Samples	Sintering method	Hardness(GPa)	Toughness(Mpa.m^(1/2))
MFA	TSS_1	6.38 ± 1.29	2.2 ± 0.82
MFA/10% Al_2O_3	TSS_2	12.39 ± 0.86	1.97 ± 0.98
MFA/ 25% Al_2O_3	TSS_2	16.62 ± 6.4	3.87 ± 1.38
MFA/ 50% Al_2O_3	TSS_2	22.09 ± 3.5	5.82 ± 1.05

Table 6: Mechanical properties of MFA/Al_2O_3 composites sintered via TSS.

days of SBF immersion (Figure 5a), the continuous reduction in Ca and P ion concentrations are associated with apatite nucleation and growth. Reportedly, fluctuations of Ca and P concentrations in SBF with immersion time (Figures 5b and 5c) are due to reduced apatite formation (corresponding to decreasing Ca and P ion concentrations) and higher dissolution of β-TCP (corresponding to increasing Ca and P ion concentrations). Furthermore, the accelerated phase dissociation is confirmed by the decrease in β-TCP intensity shown in the XRD patterns. The β-TCP dissolution after soaking HA in SBF is expressed as follows [1]:

$$4Ca_3(PO_4)_2 + H_2O \rightarrow Ca_{10}(PO_4)_6(OH)_2 + 2Ca^{2+} + 2HPO_4^{2-} \quad (2)$$

Bioactivity of magnesium fluorapatite is basically affected by the amount of dissolved β-TCP in Simulated Body Fluid (SBF).

The Mg ion concentration changes with different immersion times, as shown in Figures 6a-6c. The presence of Mg ions in SBF is due to the MFA matrix and β-TCP dissolution. It is also clear from Figure 6 that Mg ion concentration decreases with time, which could be due to the substitution of Mg ions from the SBF solution for Ca ions in calcium phosphates obtained from SBF. It has also been reported that Mg is the key factor in the formation of calcium phosphates from SBF which inhibit its precipitation in the solution [24]. It is observed that Mg ion concentration undergoes less change in the MFA/alumina composites than in pure MFA, indicating the role of alumina in preventing increased Mg content in the SBF solution.

The higher apatite on the MFA/alumina composite surfaces is due to higher bioactivity in comparison to MFA only (Figures 7 and 8). Spherical apatite particles formed on the surface is because of the surface tension and adhesion force co-effect around the crystals [13]. Covering the whole surface with spherical apatite particles is observed in composite samples with 10 and 25% alumina after 7 days of immersion in SBF (Figures 7a-7c). Moreover, there are a few spherical particles in MFA/50% alumina which are either dispersed or accumulated (Figure 7d). The accelerated nucleation and the formation of accumulated spherical particles on the surface are detected after 21 days of immersion in SBF (Figures 8a-8d). A relatively bulk apatite formed on MFA/10% alumina might be due to the accelerated apatite growth during the 21-day immersion in SBF.

Mechanical properties

It can be seen that fracture toughness and hardness of MFA/Al_2O_3 composite increased with increasing alumina. Furthermore, addition of a harder phase as alumina to MFA increased hardness. Increasing

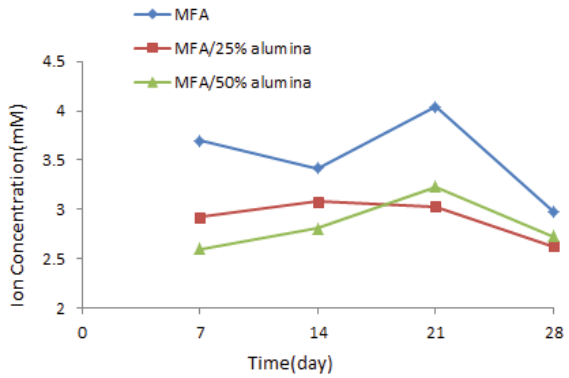

Figure 6: Changes in Mg ion concentration with immersion time for a) MFA, b) MFA/25% alumina and C) MFA/50% alumina in SBF.

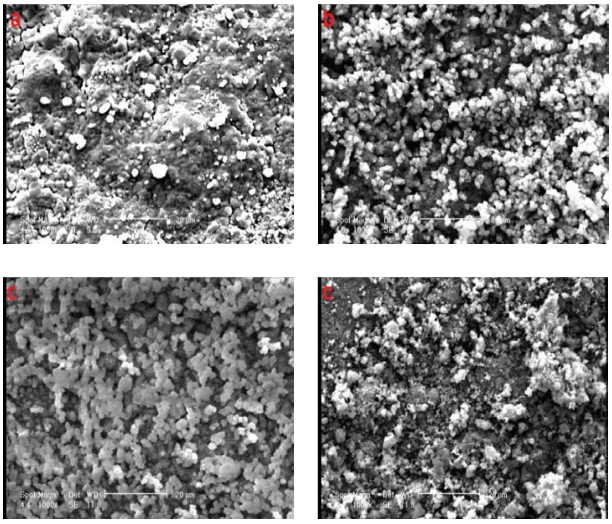

Figure 7: Apatite appearance with different morphologies for the samples a) pure MFA, b) MFA/10% alumina, c) MFA/25% alumina and d) MFA/50% alumina after 7 days immersion in SBF.

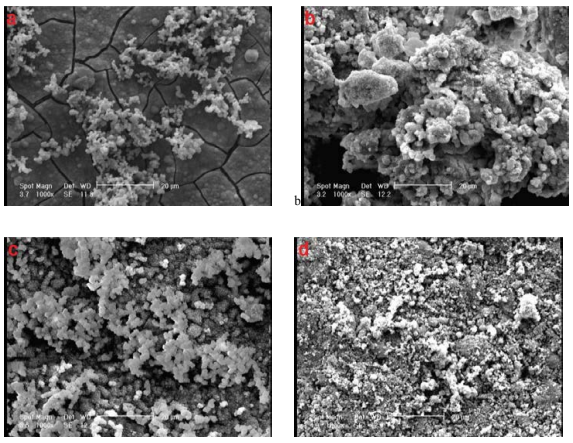

Figure 8: Surface morphologies of a) purity MFA, b) MFA/10% alumina, c) MFA/25% alumina and d) MFA/50% alumina after 21 days immersion in SBF.

in fracture toughness is due to prevention of crack growth by alumina.

Discussion

The FTIR bands and the X-ray patterns confirmed the formation of an apatite layer on the sample surfaces after 28 days of soaking in SBF. The continuous decrease in Ca and P ion concentrations indicated the nucleation and growth of apatite for MFA from 7 to 28 days of immersion in SBF. Increasing alumina content led to higher β-TCP dissolution and prevented Mg addition in the SBF solution. In all the composite samples, apatite from SBF solution was formed with the β-TCP phase. Dissolution of β-TCP increases with alumina addition. The mechanical properties (fracture toughness and hardness) of magnesium/fluorapatite were increased with alumina addition.

Acknowledgments

The authors are grateful to Isfahan University of Technology for supporting the present research.

References

1. Gu YW, Khor KA, Cheang P (2004) Bone-like apatite layer formation on hydroxyapatite prepared by spark plasma sintering (SPS). Biomaterials 25: 4127-4134.
2. Ashuri M, Moztarzadeh F, Nezafati N, Hamedani AA, Tahriri M (2012) Development of a composite based on hydroxyapatite and magnesium and zinc-containing sol-gel-derived bioactive glass for bone substitute applications. Materials Science and Engineering: C 32: 2330-2339.
3. Singh VK, Ravindra Reddy B (2012) Synthesis and characterization of bioactive zirconia toughened alumina doped with HAp and fluoride compounds. Ceramics International 38: 5333-5340.
4. Evis Z, Doremus RH (2007) A study of phase stability and mechanical properties of hydroxylapatite–nanosize a-alumina composites. Materials Science and Engineering: C 27: 421-425.
5. Hejazi MS, Ahmadian M, Meratian M, Fathi MH (2014) Effect of alumina contents on phase stability and mechanical properties of magnesium fluorapatite/alumina composites. J Mech Behav Biomed Mater 40: 95-101.
6. Nakahira A, Tamai M, Aritani H, Nakamura S, Yamashita K (2002) Biocompatibility of dense hydroxyapatite prepared using an SPS process. J Biomed Mater Res 62: 550-557.
7. Bohner M, Lemaitre J (2009) Can bioactivity be tested in vitro with SBF solution? Biomaterials 30: 2175-2179.
8. Kim HM, Himeno T, Kawashita M, Kokubo T, Nakamura T (2004) The mechanism of biomineralization of bone-like apatite on synthetic hydroxyapatite: an in vitro assessment. J R Soc Interface 1: 17-22.
9. Pierri J, Roslindo EB, Eliria RT, Agnolon Pallone MJ, Rigo E (2006) Alumina/zirconia composite coated by biomimetic method. Journal of Non-Crystalline Solids 352: 5279-5283.
10. Qi G, Zhang S, Khor KA, Liu C, Zeng X, et al. (2008) In vitro effect of magnesium inclusion in sol-gel derived apatite. Thin Solid Films 516: 5176-5180.
11. Zhang M, Liu C, Zhang X, Pan S, Xu Y (2010) Al_2O_3 /diopside ceramic composites and their behaviour in simulated body fluid. Ceramics International 36: 2505-2509.
12. Priya A, Nath S, Biswas K, Basu B (2010) In vitro dissolution of calcium phosphate-mullite composite in simulated body fluid. J Mater Sci Mater Med 21: 1817-1828.
13. Xin F, Jian C, Peng ZJ, Qian W, Cheng ZZ, et al. (2009) Bone-like apatite formation on HA/316L stainless steel composite surface in simulated body fluid. Trans Nonferrous Metal Society China 19: 347-352.
14. Baek SH, Hong SH, Cho SS, Jang DY, Joo WS (2010) Optimization of process parameters for recycling of mill scale using Taguchi experimenal design. Journal of Mechanical Science and Technology 24: 2127-2134.
15. Lourenc MA¸ Cunto GG, Figueiredo FM, Frade JR (2011) Model of two-step sintering conditions for yttria-substituted zirconia powders. Materials Chemistry and Physics 126: 262-271.
16. Aminzare M, Golestani-fard F, Guillon O, Mazaheri M, Rezaie HR (2010) Sintering behavior of an ultrafine alumina powder shaped by pressure filtration and dry pressing. Materials Science and Engineering A 527: 3807-3812.
17. Wang CJ, Huang CY, Wu YC (2008) Two-step sintering of fine alumina-zirconia ceramics. Ceramics International 35: 1467-1472.
18. Lin K, Chen L, Chang J (2012) Fabrication of dense hydroxyapatite nanobioceramics with enhanced mechanical properties via two-step sintering process. International Journal of Applied Ceramic Technology 9: 479-485.
19. Berginc B, Kampus Z, Sustarsic B (2006) The use of the Taguchi approach to determine the influence of injection-moulding parameters on the properties of green parts. Journal of Achievements in Materials and Manufacturing Engineering 15: 63-70.
20. Hidouri M, Bouzouita K, Kooli F, Khattech I (2003) Thermal behaviour of magnesium-containing fluorapatite. Materials Chemistry and Physics 80: 496-505.
21. Arockiasamy A, German RM, Wang P, Horstemeyer MF, Morgan W, et al. (2010) Sintering behaviour of Al-6061 powder produced by rapid solidification process. Powder Metallurgy. The Charlesworth Group.
22. Guidara A, Chaari K, Bouaziz J (2011) Elaboration and characterization of alumina-fluorapatite composites. JBNB 2: 103-113.
23. Obata A, Hasegawa D, Nakamura J, Jones JR, Kasuga T (2012) Induction of hydroxycarbonate apatite formation on polyethylene or alumina substrates by spherical vaterite particles deposition. Materials Science and Engineering C 32: 1976-1981.
24. Barrere F, Blitterswijk CA, Groot K, Layrolle P (2002) Nucleation of biomimetic Ca-P coatings on Ti6Al4V from a SBF × 5 solution: influence of magnesium. Biomaterials 23: 2211-2220.